https://doi.org/10.46813/2026-162-078

UDC 669.017+620.186.4

IMPROVEMENT OF QUALITY CHARACTERISTICS OF WELDED JOINTS OF NPP TURBINE ROTORS

V.V. Dmitrik[1], V.A. Belous[2], S.P. Iglin[1], A.V. Glushko[1], I.V. Kasianenko[1],
[1]National Technical University "Kharkiv Polytechnic Institute", Kharkiv, Ukraine;
[2]National Science Center "Kharkiv Institute of Physics and Technology", Kharkiv, Ukraine
E-mail: dmitrikvitali@gmail.com, tel. +38(096)0410637

To obtain welded joints of NPP turbine rotors with improved quality characteristics of their initial structure, the rotor manufacturing technology was improved. The improvement of the technology provided for the use of optimized welding mode parameters in the manufacture of rotors. Welded rotors are mainly made of 25Х2НМФА steel. The presence of structural, chemical and mechanical heterogeneity, which the metal of welded joints acquired under the influence of welding heating, gives it a corresponding susceptibility to damage under operating conditions. This susceptibility of the metal of welded joints is significantly greater compared to the similar susceptibility of the base metal of steam pipes, which was not affected by welding heating. The reduction of structural, chemical and mechanical heterogeneity was ensured by welding using mode parameters, the optimization of which was carried out on the basis of modelling of welding heating of manufactured non-separable joints. When generalizing the optimization of the modes, the thermokinetic diagram of 25Х2НМФА steel was used, and the corresponding results of experiments obtained during the manufacture of control samples were also taken into account.

INTRODUCTION

Improving the operational reliability of welded rotors of high- and intermediate-pressure turbines, namely HP and IP rotors, in relation to increasing their operating loads is becoming increasingly relevant. Such rotors are components of turbines of the K-1000-60/1500 type and their modifications, including K-1000-60/1500-2, etc. The base material of these rotors is 25Х2НМФА steel.

In the metal of welded joints manufactured using the standard technology, the presence of relatively coarse austenitic grains (grain size numbers 3–5 according to DSTU 8972:2019) and recrystallized pearlite – a new product of austenite decomposition – is observed. Such structures are formed in the fusion zone, the overheating zone, and the zone of incomplete recrystallization within the heat-affected zone (HAZ) of welded joints. To improve their quality, it is necessary to obtain austenitic grains corresponding to grain size numbers 7–9 in the fusion, overheating, and normalization regions of the HAZ. In addition, in the region of incomplete recrystallization, the new product of austenite decomposition should be obtained in the form of sorbite or troostite. These structures can be achieved by welding under optimal process parameters, the values of which were determined through simulation of the welding thermal cycles of the manufactured joints. The simulation involved solving the thermal problem in a three-dimensional coordinate system. The calculated numerical values of temperature distribution were compared with corresponding values obtained experimentally, as well as with the microstructures formed in the HAZ regions and in the weld metal.

It was taken into account that high-temperature tempering of welded joints only partially increases the resistance of austenite grain boundaries to damage formation. At the same time, during tempering, recrystallized pearlite acquires a coarsened globularized morphology, which also contributes to damage susceptibility.

Thus, optimization of process parameters in the fabrication of welded joints of turbine rotors is an extremely important task.

The aim of this work is to improve the mathematical model of the welding thermal cycle of a fabricated rotor joint made of 25Х2НМФА steel in order to obtain a welded joint with improved quality characteristics of its initial microstructure.

METHODS AND METHODOLOGY

The thermal problem was solved in a three-dimensional formulation. It was assumed that the welding process is quasi-stationary and that the weld pool shape used in the model (Fig. 1) corresponds to the actual weld pool. The thermal problem, which involved determining the welding heating and cooling of the fabricated joint (Fig. 2), was solved using the conditions of Fourier's law, taking into account the previously acquired experience reported in [1–5].

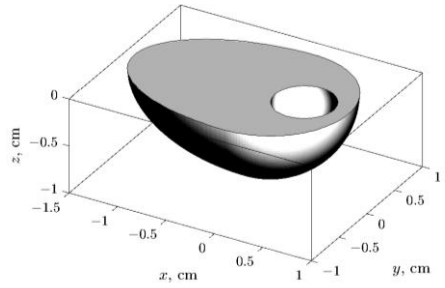


Fig. 1. Scheme of the weld pool used in the simulation of welding thermal heating

To determine the temperature regime in the molten weld pool metal and in the base metal (25Х2НМФА steel), the condition of matching boundary conditions was applied: at the interface between these regions (the fusion boundary of the HAZ), the temperature was

assumed to be T = 1500 °C. Thus, the thermal problem was solved under conditions of the combined thermal loading of the rotor welded joint (see Fig. 2).

The thermal problem was solved using the finite element method. Tetrahedral finite elements with quadratic shape functions were used. The weld pool region was divided into 47,231 elements with 68,235 nodes and a maximum element size of 0.5 mm [4], while the surrounding region was divided into 65,528 elements with 93,382 nodes and a maximum element size of 2.5 mm. This ensured sufficient accuracy of the calculated temperature values.

The temperature distribution in the weld pool shown in Fig. 1 and in the surrounding region was investigated. The solution was performed using the methodology described in [2–4]. The MATLAB mathematical package and its tools for solving partial differential equations, PDE Toolbox [4], were employed.

Optimization of the temperature regime was carried out using the thermokinetic diagram of 25Х2НМФА steel, while also taking into account temperature values determined experimentally at fixed points within the HAZ. The investigation of the structural-phase state of the welded joint metal, as well as the presence of non-metallic inclusions and defects, was performed using an MMO-1600 optical microscope and a JEOL-7100E scanning electron microscope. The studies were conducted on samples cut from the transverse section of the rotor welded joint, taking into account the previously accumulated experience [1–3].

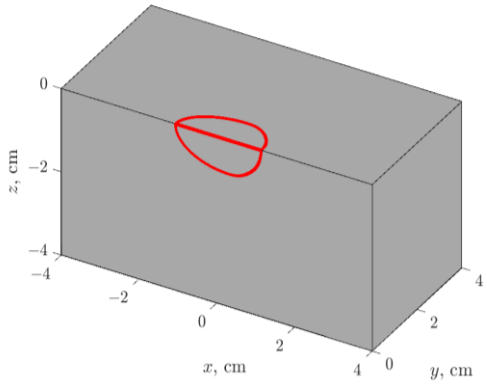


Fig. 2. Region of the thermal problem solution

The weld pool was modeled using segments of spheres, ellipsoids, and planes. It was assumed that the metal within the pool is in a liquid state, while the surrounding material remains solid. Due to symmetry, only half of the domain corresponding to positive values of the *y* coordinate was considered. This solution domain is shown in Fig. 2, where the weld pool region is highlighted. An offset of 4 cm was chosen based on the assumption that at this distance from the weld pool, the temperature approaches the preheating temperature.

The three-dimensional heat conduction problem was solved in a stationary formulation. In the absence of internal heat sources, the differential equation for this problem takes the following form:

$$div(k\,grad\,T) = 0. \qquad (1)$$

In this equation:

– T(x,y,z) – calculated temperature, K;

– x,y,z – spatial coordinates, m;

– k(x,y,z,T) – coefficient of internal thermal conductivity, W/(m·K).

For the molten weld pool in the liquid state, the internal thermal conductivity coefficient is assumed to be constant and equal to 28 W/(m·K). For solid steel, it depends on temperature. Experimental data obtained with the assistance of ChatGPT are presented in Table 1.

Table 1

Dependence of the internal thermal conductivity of solid steel on temperature

T, °C	*k*(*T*), W/(m·K)
20	30
100	28.5
200	26.5
300	24.5
400	23
500	21.5
600	19.5
1000	19
1500	19

In the calculations, spline interpolation of these data with extrapolation capability was used.

The problem was solved separately for the weld pool and for the base metal in contact with the pool. The boundary conditions were as follows:

– In the layer under the arc of the weld pool (the upper hemisphere in Fig. 1) – the Dirichlet boundary condition was applied: the temperature was assumed to correspond to the boiling point of steel, T = 3000 °C.

– At the interface between the weld pool and the solid metal, the Dirichlet boundary condition was also applied: the temperature was equal to the melting point of steel, T = 1550 °C. This condition effectively serves as the matching condition between the temperature determination in the molten weld pool and in the base metal of the HAZ.

– On the upper horizontal plane, z = 0, the Neumann boundary condition was applied to account for heat exchange with the environment according to Coulomb's law:

$$\left(k\frac{\partial T}{\partial z} + h(T - T_0) \right)\Big|_{\Gamma} = 0. \qquad (2)$$

Here h = 10 W/(m²·K) is the coefficient of external heat transfer between the steel and the air, and T_0 = 350 °C is the preheating temperature of the workpiece before welding.

– On the vertical plane y = 0, a symmetry condition was applied, which also serves as a Neumann boundary condition (perfect thermal insulation):

$$\left.\frac{\partial T}{\partial y}\right|_{\Gamma} = 0. \qquad (3)$$

– On all other boundaries, Dirichlet boundary conditions were applied: the temperature was set equal to the preheating temperature of the workpieces before welding, T = 350 °C.

Figs. 3 and 4 show the temperature distribution in the weld pool. Fig. 5 presents the temperature distribution in the heat-affected zone (HAZ), while Figs. 6 and 7 illustrate the temperature distribution in its sections.

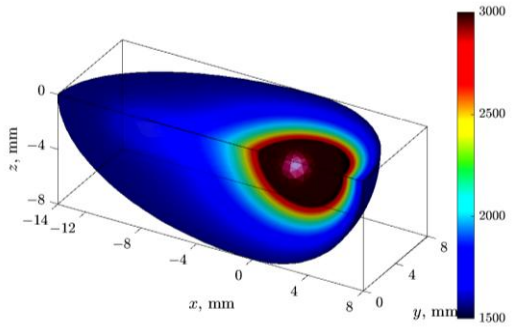


Fig. 3. Temperature distribution in the weld pool

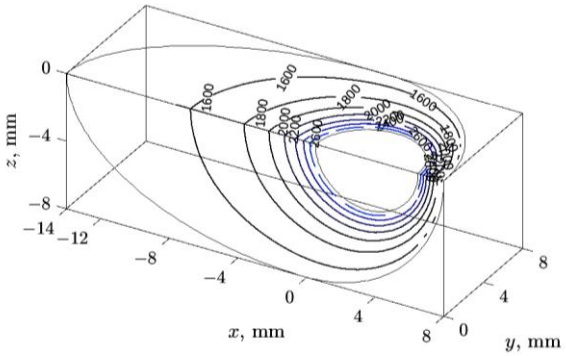


Fig. 4. Temperature distribution in the weld pool

RESULTS AND DISCUSSION

The temperature regime for both the molten weld pool metal and the base metal was determined according to Fourier's law. Thus, by means of simulation, the temperature distribution in the fabricated rotor welded joint was obtained (see Figs. 2, 5).

By solving the thermal problem using the finite element method, the required temperature regime in the fabricated rotor welded joint was successfully achieved.

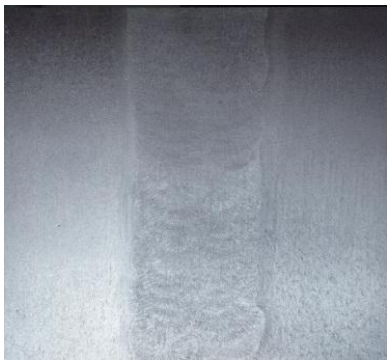


Fig. 5. Macrosection of the welded joint made of 25Kh2NMFA steel, ×1.1

When solving this thermal problem, it is advisable to choose a system of basis functions $\{\varphi_i\}$ with respect to which the expansion is performed and to represent them in the form of polynomials. This approach made it possible to project the obtained solution expansions onto an n-dimensional subspace corresponding to a linearly independent system of basis functions $\{\psi_i\}$, (i = 1, 2, …, n). The projection method allowed the formation of densely populated matrices of relatively small size, which ensured the determination of the required temperature values in the regions of the HAZ of the welded joints. Since the selection of the initial basis functions was based on experimental data, the calculated temperature values in the weld metal were characterized by sufficient accuracy.

The obtained isotherms, which describe the temperature fields in the welded joints, depend on heat transfer from the volume of the weld pool, which in turn depends on the welding process parameters. Thus, solving thermal problem (1) made it possible to establish the conditions that characterize the corresponding formation of the weld metal structure and the HAZ regions (Figs. 3, 4, 7, 8) with enhanced quality characteristics.

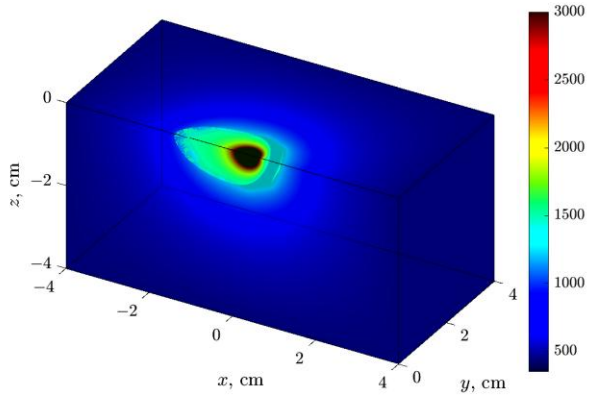


Fig. 6. Fragment of the temperature distribution during welding thermal cycles (see Fig. 5)

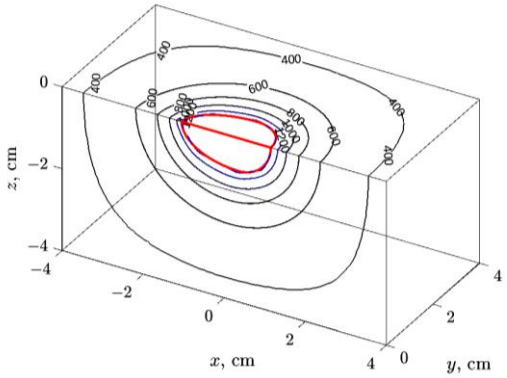


Fig. 7. Fragment of the temperature distribution during welding thermal cycles (see Fig. 5)

By solving the thermal problem, the required temperature regime in the fabricated rotor welded joint was achieved. The solution of the thermal problem allowed:

1. Determination of the temperature regime by calculation, under which the base microstructure of the weld metal is formed with enhanced quality characteristics.

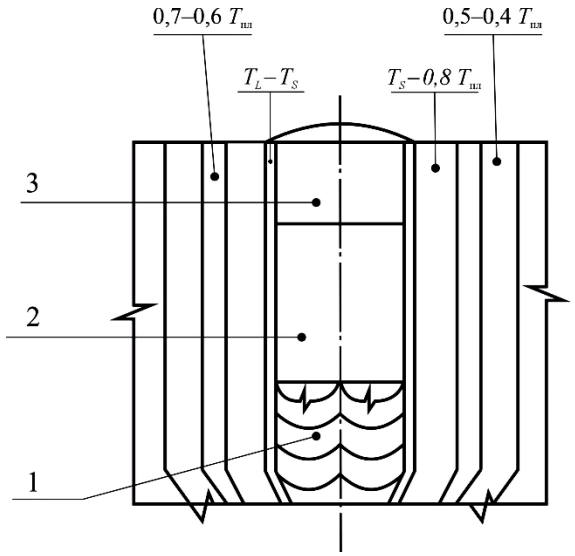


Fig. 8. Scheme of the calculated temperatures in the rotor welded joint: 1 – Lower weld zone; 2 – Middle zone; 3 – Upper zone

2. Using the calculated temperature field data, it was possible to optimize the parameters of the automatic welding process.

3. Reduce the overall level of initial structural heterogeneity in the metal of the fabricated welded joints.

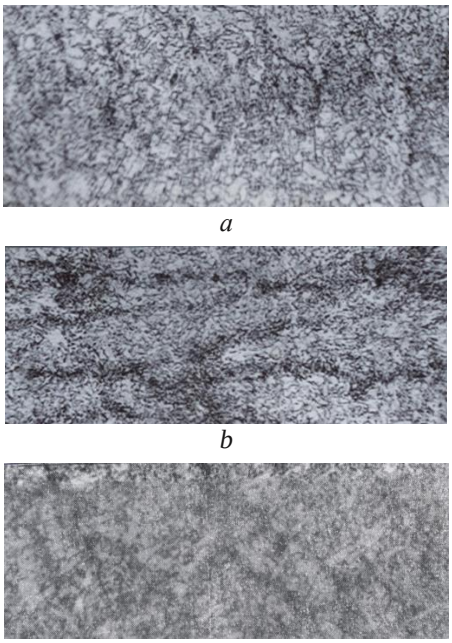
4. Solving the thermal problem in a three-dimensional coordinate system has significant advantages over a similar solution in cylindrical coordinates [3]. It allows obtaining more accurate calculated temperature values throughout the volume of the welded joint. The actual shape of the weld pool does not always correspond well to cylindrical coordinates when welding parameters are varied. This discrepancy can lead to, in certain regions of the HAZ, temperature values that do not fully match experimental measurements.

RESEARCH RESULTS

The use of temperature regime modeling allowed the establishment of a thermal regime that ensures the formation of the base microstructure of the welded joint with enhanced quality characteristics (Fig. 9). Determining the temperature regime enabled the optimization of welding process parameters, including welding current, arc voltage, welding speed, electrode wire feed rate, and wire diameter. On templates cut from the welded joint, following the procedure in [1], the microstructure, chemical composition, and properties were investigated.

The welding materials used were the same as those applied previously [1]. Preheating and interpass heating during the fabrication of the welded joint were maintained at 350 °C. The welded joints were subjected to tempering immediately after welding at 600 °C for 130 h.

To assess the reliability of the welded joint, its base microstructure was examined, and the mechanical properties were determined on samples cut from the corresponding zones of the joint (see Fig. 8). It was recognized that the operational reliability of welded joints under increased working stresses largely depends on the structural-phase state of the weld metal [5–7]. Therefore, the base microstructure of the welded joints was studied separately on samples from zones 1, 2, and 3. In the same manner, the mechanical properties were determined separately. The analysis also took into account the temperature field distribution in the fabricated joints with respect to the formation of their metal microstructure.



a

b

c

Fig. 9. Microstructure of the weld metal in the welded joint (see Fig. 8): a – Weld metal of zone 1; b – Zone 2; c – Zone 3, ×400

The improvement of the overall welding technology was largely aimed at preventing the formation of coarse austenitic grains in the fusion, overheating, and normalization regions of the HAZ. The size of the austenitic grains depends on the heating of the HAZ metal into the Ts–Ac_3 temperature range, and therefore it is advisable to minimize the residence time of the HAZ metal in this temperature range. At the same time, precautions were taken to prevent defects such as lack of fusion along the gap walls and lack of fusion between passes. Consideration was also given to the possibility of accumulation of chemical compounds and harmful elements at austenite grain boundaries, which can promote damage formation along these boundaries. For the first time, a feature of the dependence of new austenite decomposition products on the temperature regime was established in the region of incomplete HAZ recrystallization, forming in the form of sorbite or troostite.

It was demonstrated that welding under optimized process parameters allows the formation of new austenite decomposition products in the form of sorbite and troostite (Fig. 10), instead of pearlite.

The studies showed that the weld metal microstructure in zones 1–3 of the welded joint (see Fig. 8) consists of tempered bainite and ferrite, as illustrated in Fig. 9.

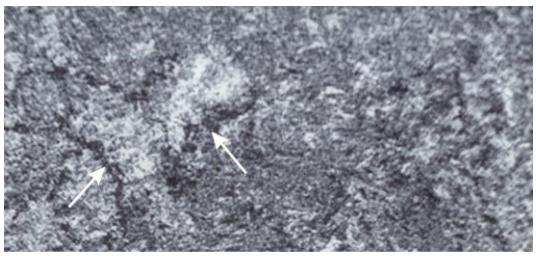


Fig. 10. Microstructure of the HAZ incomplete recrystallization region. New austenite decomposition products located at austenite grain boundaries (arrows) represent sorbite, ×400

Secondary phases in varying proportions are distributed throughout the bodies of the bainite and ferrite grains. The fusion zone of samples cut from zones 1–3 is characterized by a predominantly smooth transition of the weld metal microstructure into the base metal structure. In the weld metal of the sample from zone 2, an increased amount of ferrite grains was observed compared to the samples from zones 1 and 3 (Fig. 11).

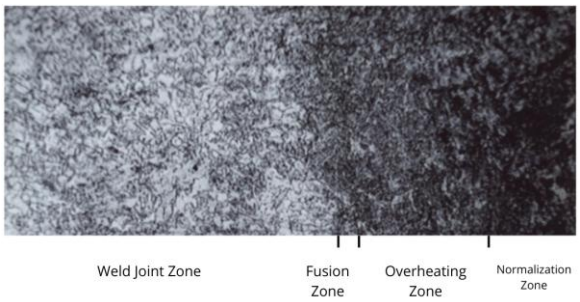


Fig. 11. Microstructure of the welded joint, zone 2 (see Fig. 4), ×400

The overheating regions of the HAZ (Fig. 12) in samples from zones 1–3 (see Fig. 8) exhibit a sorbite–troostite microstructure. In samples from zones 1 and 3, a higher proportion of sorbite is noted compared to the structure of the sample from zone 3.

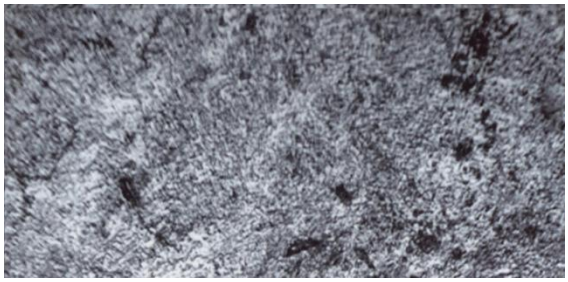


Fig. 12. Microstructure of the HAZ overheating region of the welded joint, zone 2 (see Fig. 8), ×400

In the normalization regions of the HAZ, the microstructures also showed minor differences. The incomplete recrystallization regions of the HAZ in samples from zones 1–3 are characterized by the presence of new austenite decomposition products in the form of sorbite (see Fig. 10), while the structure of the sample from zone 2 is troostite. Thus, fabrication of welded joints under optimized welding parameters made it possible to obtain new austenite decomposition products as sorbite and troostite, while preventing the formation of pearlite as a new austenite decomposition product.

The microhardness measurements confirm the presence of these structures in samples from zones 1–3 of the welded joint.

The widths of the HAZ regions were determined (Table 2), as well as the presence of austenitic grains in these regions (Table 3).

Table 2

Width (mm) of the HAZ regions in samples 1–3 (see Fig. 8)

Weld Joint Zone	Fusion Zone	Overheating Zone	Normalization Zone
1	0.1	1.3	1.2
2	0.15	1.9	1.7
3	0.1	1.3	1.2

Table 3

Average austenite grain size in the HAZ regions of samples 1–3 (see Fig. 8), according to DSTU 8972:2019

Weld Joint Zone	Fusion Zone	Overheating Zone	Normalization Zone
1	6	7	8
2	7	8	9
3	6	7	8

The determination of the mechanical properties of samples 1–3 (see Fig. 8) showed relatively small differences in their values (Table 4), which overall meet the regulatory requirements and, in some cases, are slightly higher.

It was demonstrated that modeling the welding thermal cycles of the fabricated joints allowed the optimization of welding process parameters and the production of welded joints with enhanced quality characteristics of their base microstructure. The simulation of welding thermal cycles enabled the improvement of the automatic welding technology for high-power turbine rotors made of 25Х2НМФА steel.

Considering the features of microstructure formation under the influence of welding thermal cycles in the fabricated welded joints (see Figs. 8–12, [7–8]) is essential for the development of new steels and welded joints made from these steels, which are capable of withstanding higher operational loads than analogous welded joints made of 25Х2НМФА steel.

Table 4

Mechanical properties of samples 1–3 (see Fig. 8)

Weld Joint Zone	Ultimate Strength, N/mm²	Yield Strength, N/mm²	Elongation, %	Reduction of Area, %	Impact Toughness, J/cm²	Hardness, HB
1	790	530	25	64	186	198
2	770	510	28	67	184	193
3	780	540	24	63	184	197

Note. A V-shaped notch was made at the middle of the weld metal.

CONCLUSIONS

1. It was established that solving the three-dimensional thermal problem during simulation of welding thermal cycles allows for increased accuracy in the temperature field distribution within the rotor welded joint.

2. The use of temperature field data in the welded joint during fabrication made it possible to refine the previously established parameters of the automatic welding process.

3. It was determined that the automatic welding of a rotor made of 25Х2НМФА steel under the proposed process parameters enables the formation of a base microstructure of welded joints with improved quality characteristics and enhanced mechanical properties compared to welded joints produced using standard technologies.

4. It was demonstrated that in the incomplete recrystallization region of the HAZ, new austenite decomposition products form at austenite grain boundaries in the form of pearlite, sorbite, or troostite. For the first time, it was established that welding under optimized process parameters ensures the formation of new austenite decomposition products specifically as sorbite or troostite.

REFERENCES

1. V.V. Dmitrik, V.Yu. Skulsky, I.V. Kasyanenko, O.V. Vavilov, O.G. Kantor. Improving the quality condition of the structure of welded joints made of rotor steel // *Problems of Atomic Science and Technology*. 2022, N 2(138), p. 87-91; https://doi.org/10.46813/2022-138-087

2. О.К. Морачковський, В.В. Дмитрик, О.П. Усатий, Б.П. Зайцев, В.Ю. Скульский, М.М. Гришин. *Створення роторів турбін великої потужності*: Монографія. Харків, 2019, 250 с.

3. V.V. Dmitrik, A.V. Glushko, I.V. Kasianenko, T.O. Syrenko, T.A. Baranova, I.V. Asieieva. Improvement of welding technology of high power turbine rotor // *Problems of Atomic Science and Technology*. 2024, N 2(150), p. 121-124; https://doi.org/10.46813/2024-150-121

4. С.П. Іглін, В.В. Дмитрик, В.Ю. Скульський. Моделювання руху рідкого металу в зварювальній ванні // *Електронне моделювання*. 2020, № 1, с. 51-71; https://doi.org/10.15407/emodel.42.01.051

5. V.V. Dmitrik, Chen Xinlei, I.V. Kasianenko, I.B. Ustyuzhyn. Improving the output quality of steam turbine welded rotors for nuclear power plants // *Problems of Atomic Science and Technology*. 2025, N 2(156), p. 91-95; https://doi.org/10.46813/2025-156-091

6. И.А. Борисов, А.В. Дуб. Влияние продолжительности высокого отпуска на текстуру и зерно перегретой роторной стали // *Металловедение и термическая обработка металлов*. 2013, №3, с. 3-9.

7. A.V. Semenov, A.A. Kozlovskyi, S.N. Skorik, D.V. Lubov. Gas Sensing Properties of Nanocrystalline Silicon Carbide Films: Experimental Results // *Innovations in Science and Technology*. 2022, v. 5, p. 18-25; https://doi.org/10.9734/bpi/ist/v5/1816B

8. L.M. Lobanov, V.A. Kostin, O.V. Makhnenko, V.V. Zukov, E.S. Kostenevich. Forecasting of structural transformations in heat affected zone steel of 15KH2NMFA at anti-corrosion cladding // *Problems of Atomic Science and Technology*. 2020, N 2(126), p. 89-96.

Article received 19.03.2026

ПІДВИЩЕННЯ ЯКІСНИХ ХАРАКТЕРИСТИК ЗВАРНИХ З'ЄДНАНЬ РОТОРІВ ТУРБІН АЕС

В.В. Дмитрик, В.А. Білоус, С.П. Іглін, А.В. Глушко, І.В. Касьяненко

Для отримання зварних з'єднань роторів турбін АЕС із підвищеними якісними характеристиками їх вихідної структури удосконалювали технологію виготовлення роторів. Удосконалення технології передбачало використання при виготовленні роторів оптимізованих параметрів режиму зварювання. Зварні ротори переважно виготовляють зі сталі 25Х2НМФА. Наявність структурної, хімічної і механічної неоднорідностей, що набув метал зварних з'єднань під впливом зварювального нагрівання, надає йому відповідну схильність до пошкоджуваності в умовах експлуатації. Така схильність металу зварних з'єднань є значно більшою порівняно з аналогічною схильністю основного металу паропроводів, який не зазнав впливу зварювального нагрівання. Зменшення структурної, хімічної і механічної неоднорідностей забезпечено шляхом зварювання з використанням параметрів режиму, оптимізацію яких здійснено на основі моделювання зварювального нагрівання виготовляємих нероз'ємних з'єднань. При узагальнені оптимізації режимів використовували термокінетичну діаграму сталі 25Х2НМФА, а також враховували відповідні результати експериментів, отриманих при виготовленні зразків-свідків.